

Phys. Soc. 7, 187 (1962); P. H. Carr and M. W. P. Strandberg, *J. Phys. Chem. Solids* 23, 923 (1962); A. L. Taylor and G. W. Farrell, *Can. J. Phys.* 42, 595 (1964); H. E. Weaver and P. Schindler, *Nature* 51, 82 (1964); S. T. Wang and G. W. Farrell, *Can. J. Phys.* 43, 1919 (1965); Kh. I. Zil'bershtein, V. A. Ioffe, and Yu. F. Fedorov, *Kristallografiya* 10, 727 (1965) [*Sov. Phys. Crist.* 10, 607 (1966)]; M. F. Lewis, H. M. Rosenberg, and J. K. Wigmore, *Phys. Status Solidi* 15, 317 (1966); R. A. Weeks, *J. Am. Chem. Soc.* 53, 176 (1970); R. Schandt and J. Schneider, *Physik Kondensierten Materie* 11, 19 (1970); J. H. Mackey, J. W. Boss, and D. E. Wood, *J. Magnetic Res.* 3, 44 (1970).

³J. H. Anderson and J. A. Weil, *J. Chem. Phys.* 31, 427 (1959); *Bull. Am. Phys. Soc.* 3, 135 (1958); 4, 284 (1959); 4, 416 (1959); Y. Haven, A. Katz, and J. S. Van Wieringen, *Philips Res. Rept.* 21, 446 (1966); in *Proceedings of the Eleventh Colloque Ampère* (North-Holland, Amsterdam, 1963), p. 403; *Verres Refractaires* 12, 191 (1958), F. J. Fiegl and J. H. Anderson, *J. Phys. Chem. Solids* 31, 575 (1970); *Bull. Am. Phys. Soc.* 9, 654 (1964); J. A. Weil and J. H. Anderson, *J. Chem. Phys.* 35, 1410 (1961).

⁴D. R. Hutton, *Phys. Letters* 12, 310 (1964); T. I. Barry and W. J. Moore, *Science* 144, 289 (1964); T. I.

Barry, P. McNamara, and W. J. Moore, *J. Chem. Phys.* 42, 2599 (1965); G. Lehmann and W. J. Moore, *ibid.* 44, 1741 (1966); L. M. Matarrese, J. S. Wells, and R. L. Peterson, *ibid.* 50, 2350 (1969); *Bull. Am. Phys. Soc.* 9, 502 (1964); *Natl. Bur. Std. (U. S.) Tech. Note* 372, 1969 (unpublished); A. R. Cook and L. M. Matarrese, *J. Chem. Phys.* 50, 2361 (1969).

⁵P. M. Wright, J. A. Weil, T. Buch, and J. H. Anderson, *Nature* 197, 246 (1963); H. Rinneberg and J. A. Weil (unpublished).

⁶J. A. Weil, *J. Chem. Phys.* (to be published).

⁷M. H. Cohen, D. A. Goodings, and V. Heine, *Proc. Phys. Soc. (London)* 73, 811 (1957); V. Heine, *Czech. J. Phys.* B13, 619 (1963); *Phys. Rev.* 107, 1002 (1957); D. A. Goodings, *ibid.* 123, 1706 (1961); T. P. Das and A. Mukhenji, *J. Chem. Phys.* 33, 1808 (1960).

⁸J. D. Weeks, A. Hazi, and S. A. Rice, *Advan. Chem. Phys.* XVI, 283 (1969).

⁹The 4s orbital of the Ge¹⁺ ion is used in our calculation, since our calculation is approximate.

¹⁰E. Fermi, *Z. Physik* 60, 320 (1930).

¹¹Arnold C. Wahl, P. J. Bertoncini, K. Kaiser, and Robert H. Land, AEC Research and Development Report No. ANL-7271 (unpublished).

Hyperfine Interactions of ⁵⁷Fe in Fe₃C[†]

M. Ron

Department of Materials Engineering, Technion—Israel Institute of Technology, Haifa, Israel

and

Z. Mathalone*

Department of Physics, Technion—Israel Institute of Technology, Haifa, Israel

(Received 4 March 1971)

The absence of the quadrupole interaction from the room-temperature spectrum of Fe₃C is shown to be only apparent. The spectrum was unfolded into two components in accordance with the two known structural sites, G (general) and S (special). The electric field gradient is found to be axially symmetric at each site. The quadrupole interaction is found to be 0.32 mm/sec for the G site and -0.58 mm/sec for the less-symmetric S site. The angles θ between the magnetic field \vec{H} and the electric field gradient V_{zz} were found to be 50° and -50° for G and S, respectively. The hyperfine fields are found to be $H_G = 205$ kOe and $H_S = 207$ kOe. No difference in the isomer shift could be observed. The only indications of two sites in the room-temperature spectrum are the broadening (and therefore shortening) of the $+\frac{3}{2} \rightarrow +\frac{1}{2}$ transition line (sixth line), and a smaller broadening of the $-\frac{1}{2} \rightarrow -\frac{3}{2}$ transition line (second line).

INTRODUCTION

The χ -iron carbide Fe₅C₂ has been widely studied.^{1,2} It is monoclinic and has the space group C₂/2. The iron atoms occupy two sets of eightfold general positions (type I and II) and one fourfold set (type III).

In accordance with the structure determination by Fasiska and Jeffrey,³ the θ -iron carbide Fe₃C (cementite) is orthorhombic and has the space

group P_{nma}. The iron atoms are located in two types of sites. An iron atom Fe_G at the general G site has 3 C and 11 Fe nearest neighbors in a less-symmetric arrangement than an iron atom, Fe_S, at the special S site with 2 C and 12 Fe nearest neighbors.

The two carbides have been widely studied by the Mössbauer effect. The Mössbauer spectrum of the χ carbide has been shown to have a fine structure due to the different sites of the iron atoms.⁴

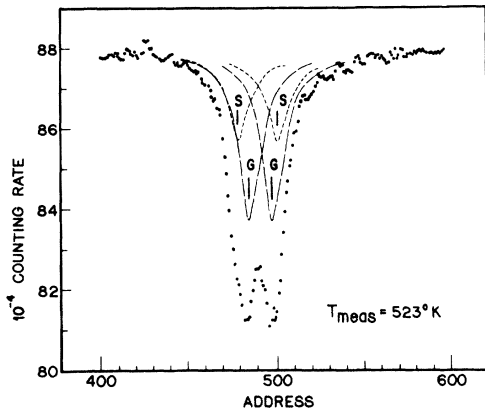


FIG. 1. Mössbauer spectrum of Fe_3C above the Curie temperature. The broken lines represent the assumed Fe_C and Fe_S components.

The Mössbauer parameters of synthesized^{4,5} Fe_3C , extracted from tempered steel^{6,7} or inside a steel matrix,⁷⁻¹⁰ are known. No fine structure has, so far, been indicated in the spectra of Fe_3C taken at temperature $T < T_C$, where T_C is the Curie Temperature.

In this study the spectrum of Fe_3C (at $T < T_C$) is unfolded into two components, G and S, related to iron atoms at general and special sites.

EXPERIMENTAL

An Fe-C alloy of approximately eutectoid composition was cast. After the alloy was hot forged, it was homogenized at 1050 °C in a protective atmosphere. The precipitation of the cementite was done by tempering the alloy at 650 °C for 5 h.

The cementite was extracted chemically from the matrix by a process described elsewhere.¹¹ The residual powder, which was used as a Mössbauer absorber, was identified by x-ray diffraction as Fe_3C . The absorber thickness was $\sim 15 \text{ mg/cm}^2$ of Fe.

The Mössbauer spectra were taken by a constant-velocity spectrometer.¹² The velocity scale was calibrated by means of an Armco iron absorber.¹³ The linewidth of the $\mp \frac{3}{2} \rightarrow \mp \frac{1}{2}$ transition lines (lines 1 and 6) of this absorber was about 0.32 mm/sec. A 15-mCi radioactive source of ^{57}Co in palladium matrix was used throughout the experiments.

RESULTS AND INTERPRETATION

A spectrum, taken at 250 °C above the Curie temperature of Fe_3C , is shown in Fig. 1. The spectrum fits two superimposed quadrupole-split Lorentzian lines which have the following hyperfine parameters:

$$(Q_S)_C = 0.32 \text{ mm/sec}, \quad (S_I)_C = 0.00 \text{ mm/sec},$$

$$(Q_S)_S = -0.58 \text{ mm/sec}, \quad (S_I)_S = -0.08 \text{ mm/sec},$$

where Q_S is the quadrupole-splitting term and S_I is the isomer shift. The S_I are relative to α -iron.

The linewidth is taken to be $\Gamma = 0.38 \text{ mm/sec}$ and the intensity ratio $I_C : I_S$ is constrained to have the value 2 : 1. The intensities of each pair of quadrupole lines are assumed to be symmetrical because the Goldanskii-Karyagin anisotropy effects are not expected. In fact, no change in the symmetry of the line intensities with ambient temperature has been observed.¹¹ At room temperature, cementite is below its Curie temperature ($T_C \approx 210 \text{ °C}$). A typical room-temperature spectrum of Fe_3C is shown in Fig. 2. The inner lines ($\pm \frac{1}{2} \rightarrow \mp \frac{1}{2}$) are superimposed on a small amount of oxyhydroxide owing to the process of the preparation of the material.¹¹ The hyperfine parameters of this phase are given elsewhere.¹¹ The experimental data were assumed to be a superposition of two six-peak Zeeman patterns G and S as indicated by the arrows. Their hyperfine parameters are given in Table I.

Expected Mössbauer spectra for ^{57}Fe have been computed by Kundig¹⁴ for any given combination of magnetic field \vec{H} and electric field gradient (efg). The Hamiltonian of a state for a dipole transition $\frac{3}{2} \rightarrow \frac{1}{2}$ is taken as a sum of the magnetic interaction H_m and the electric quadrupole interaction H_Q . The z direction is chosen as the direction of the efg component $V_{zz} = \partial^2 V / \partial z^2$. The transition energies $E(\frac{3}{2}, i; \frac{1}{2}, j)$ and intensities are calculated and plotted for any given combination of \vec{H} , $e^2 Q V_{zz}$, η , θ , and φ . Here, e is the proton charge, η the asymmetry parameter, and θ and φ the polar and azimuthal angles, respectively, of \vec{H} with respect to the V_{zz} axis.

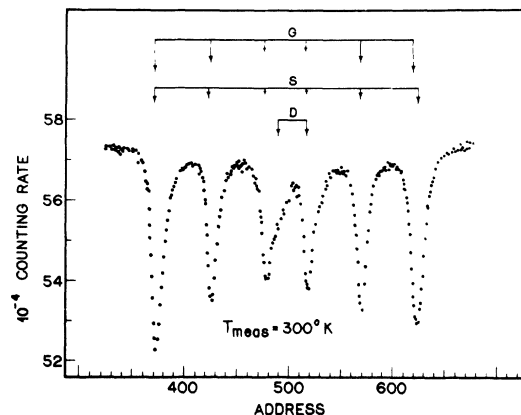


FIG. 2. Room-temperature Mössbauer spectrum of Fe_3C below the Curie temperature. The arrows assigned G and S indicate the position and relative intensities of the assumed Fe_C and Fe_S components.

TABLE I. Hyperfine parameters of the G and S components at room temperature.

Site	H (kOe)	S_I^a (mm/sec)	Q_S^b (mm/sec)	I (relative)	Γ^c mm/sec
G	205	0.17 ± 0.02	0.32 ± 0.04	2	0.26 ± 0.04
S	207	0.17 ± 0.02	-0.58 ± 0.04	1	0.26 ± 0.04

^aRelative to α -iron.

^b $Q_S = \frac{1}{2} e^2 q Q (1 + \frac{1}{3} \eta^2)^{1/2}$.

^cLinewidth at half-maximum (LWHM) of the $-\frac{3}{2} \rightarrow -\frac{1}{2}$ lines.

In the graphs, the line position, line intensities, and isomer shifts are plotted as functions of

$$|R| = \left| \frac{1}{2} e^2 q V_{zz} / g_{3/2} IH \right|,$$

where g and I are the nuclear g factor and spin, respectively. By fitting a measured and normalized spectrum to one of the graphs, the angles φ and θ , the parameter η , and R (including its sign) can be obtained. This procedure is useful for a single six- (or eight-) line spectrum.

The spectrum in Fig. 2 was treated as consisting of two hyperfine-split six-line spectra (designated G and S). The values of $(Q_S)_G$ and $(Q_S)_S$ as derived from the measurements at $T > T_C$ were used for the determination of

$$R_G = \frac{1}{2} e^2 q V_{zz}^G / g_I H, \quad R_S = \frac{1}{2} e^2 q V_{zz}^S / g_I H,$$

where G and S refer to general and special sites occupied by an iron atom. In this first approximation a mean value of $H = 207$ kOe was used, which was determined from the unresolved spectrum of Fe_3C .

With these values of R_G and R_S , the hyperfine parameters of two test spectra were obtained. Using the constraint that the intensity ratio is $I_G : I_S = 2 : 1$, by trial and error a best fit of the superimposed spectrum with the experimental results was achieved. The only combination which gave good agreement with the data was $\eta = 0$ and $\varphi = 0$ for both G and S components, i. e., the efg has axial symmetry at the two sites. The angles between the directions of H and V_{zz}^G , and H and V_{zz}^S were found to be $\theta_G = 50^\circ$ and $\theta_S = -50^\circ$. The negative sign indicates that the two V_{zz} axes point in opposite directions.

The corrected values of R obtained by the above fit are $R_G = 0.23$ and $R_S = 0.41$. The evaluated hyperfine parameters are specified in Table I.

DISCUSSION

The quadrupole interaction determined at $T > T_C$ of the Fe_S atoms is almost twice that of the Fe_G atoms. This probably results from the fact that the

Fe_G atoms occupy a more symmetric site.³ The degree to which the quadrupole interaction influences the line positions of a spectrum taken at $T < T_C$ (i. e., in the presence of the magnetic interaction) depends on the angle θ .

When the symmetry axis of an axially symmetrical tensor of the efg is at an angle $\theta \neq 0$ or π to the direction of the magnetic field H , then for $I_{ex} = \frac{3}{2}$, the eigenvalues of the Hamiltonian are

$$E_m = -(\mu/I) mH + (-1)^{|m|+1/2} \frac{1}{6} e^2 q V_{zz} (3 \cos^2 \theta - 1),$$

where μ is the nuclear magnetic moment.

The angles θ_G and θ_S , which correspond to the Fe_G and Fe_S sites, were found to be 50° and -50° , respectively. For these values of θ the factor $3 \cos^2 \theta - 1$ equals 0.23 and therefore the asymmetry in the positions due to the quadrupole interaction is small.

The difference in the hyperfine fields H_G and H_S is of the order of 1% and the isomer shifts are close. Therefore, the corresponding two six-line patterns are similar. The only pronounced features of the spectrum of Fe_3C at $T < T_C$ are the shortened and broadened sixth line and somewhat broadened second line. The sixth line consists of two $+\frac{3}{2} \rightarrow +\frac{1}{2}$ transitions (of the G and S) 0.11 mm/sec apart, and the second line consists of two $-\frac{1}{2} \rightarrow -\frac{3}{2}$ transitions 0.02 mm/sec apart.

Thus, the absence of the fine structure from the spectrum of Fe_3C at $T > T_C$ due to the quadrupole interaction and the two structural sites Fe_G and Fe_S as was mentioned by Huffman *et al.*⁵ and Bernas *et al.*⁴ is apparent only. In fact the spectrum is unfolded into two six-line spectra displaying two different magnetic and electric quadrupole interactions in accordance with the two structural sites Fe_G and Fe_S .

The Mössbauer analysis has been used for the identification of phases which appear in steels in the process of annealing. For this purpose, the knowledge of the fine structure of the spectrum of Fe_3C and other carbides is indispensable. The identification of χ carbide by the broadened and shortened sixth-line transition ($+\frac{3}{2} \rightarrow +\frac{1}{2}$) as is sometimes done⁸ may lead to erroneous conclusions.

The relatively small disagreement between the Q_S and S_I , measured at $T > T_C$, of this study and those of Huffman *et al.*⁵ may be caused by the admixture of iron present in their samples, or associated with differences in data-fitting constraints.

ACKNOWLEDGMENT

Recomputed tables in an enlarged form were kindly supplied by W. Kundig, Department of Physics, University of California.

[†]Work sponsored by the U. S. National Bureau of Standards.

*In partial fulfillment of the requirements for the D. Sc. degree.

¹K. H. Jack and S. Wild, *Nature* **212**, 248 (1966).

²M. J. Duggin and L. J. E. Hofer, *Nature* **212**, 248 (1966).

³E. J. Fasiska and G. A. Jeffrey, *Acta Cryst.* **19**, 463 (1965).

⁴H. Bernas, I. A. Campbell, and R. Fruchart, *J. Phys. Chem. Solids* **28**, 17 (1967).

⁵G. P. Huffman, P. R. Errington, and R. M. Fisher, *Phys. Status Solidi* **22**, 473 (1967).

⁶T. Shinjo, F. Itoh, M. Takaki, Y. Nakamura, and N. Shikazono, *J. Phys. Soc. Japan* **19**, 1252 (1964).

⁷M. Ron, H. Shechter, and S. Niedzwiedz, *J. Appl. Phys.* **39**, 265 (1968); H. Shechter and M. Ron, *Nucl. Phys.* **A109**, 588 (1968).

⁸H. Ino, T. Moriya, F. E. Fujita, Y. Maeda, Y. Ono, and Y. Inokuti, *J. Phys. Soc. Japan* **25**, 88 (1968).

⁹B. W. Christ, P. M. Giles, *Trans. AIME* **242**, 1915 (1968).

¹⁰P. M. Gielen and R. Kaplow, *Acta Met.* **15**, 49 (1967).

¹¹Z. Mathalone, M. Ron, J. Pipman, and S. Niedzwiedz, *J. Appl. Phys.* **42**, 687 (1971).

¹²J. Lipkin, B. Shechter, S. Shtrikman, and D. Treves, *Rev. Sci. Instr.* **35**, 1336 (1964).

¹³H. Shechter, M. Ron, and R. H. Herber, *Nucl. Instr. Methods* **44**, 268 (1966).

¹⁴W. Kundig, *Nucl. Instr. Methods* **48**, 219 (1967).

Infrared Absorption and Luminescence Spectra of Fe^{2+} in Cubic ZnS: Role of the Jahn-Teller Coupling

Frank S. Ham and G. A. Slack

General Electric Research and Development Center, Schenectady, New York 12301

(Received 10 March 1971)

A revised interpretation of the ${}^5E \rightarrow {}^5T_2$ optical absorption spectrum of Fe^{2+} in cubic ZnS is proposed. It is shown that certain absorption peaks, lacking a counterpart in the luminescence, cannot be interpreted, as previously done, as two- and three-phonon sidebands of the zero-phonon transitions, and also cannot be attributed to crystal-field electronic transitions or to simple unshifted one-phonon sidebands. A Jahn-Teller coupling within the 5T_2 level, weaker than the spin-orbit coupling, is shown to be capable not only of partially quenching the 5T_2 spin-orbit splitting but also of shifting the associated one-phonon levels in the manner required to account for the observed spectra. Such a dynamic Jahn-Teller effect, involving simultaneous coupling to a low-frequency mode ($\sim 100 \text{ cm}^{-1}$) and a higher-frequency mode ($\sim 300 \text{ cm}^{-1}$), is proposed to account for the data for Fe^{2+} in ZnS in terms of coupling to the TA and TO and/or LO phonons of the ZnS lattice. This interpretation of the phonon coupling is shown to be consistent with a moment analysis of the broadening of the optical absorption and luminescence spectra using the methods of Henry, Schnatterly, and Slichter. The relation of this model to similar features in the spectrum of Fe^{2+} in CdTe, MgAl_2O_4 , ZnSe, ZnTe, CdS, GaP, and GaAs is discussed. It is also shown that this model provides insights into the relationship between lattice phonons and the localized modes that dominate the Jahn-Teller coupling in strongly coupled systems, and that it shows why the cluster model for the Jahn-Teller ion and its nearest neighbors often works well for such systems.

I. INTRODUCTION

The optical absorption spectrum in the near infrared of the Fe^{2+} ion in cubic ZnS, CdTe, and MgAl_2O_4 has been studied by Slack, Ham, and Chrenko (SHC).¹ It was found that the structure in these spectra, which correspond to the ${}^5E \rightarrow {}^5T_2$ transition, was not in agreement with the predictions of simple crystal-field (or ligand-field) theory for Fe^{2+} in a tetrahedral site. The dynamic Jahn-Teller effect was shown to offer a possible explanation for these discrepancies, and for ZnS: Fe^{2+} a phenomenological model involving strong Jahn-Teller coupling in the 5T_2 state was proposed which fit quantitatively the observed zero-phonon struc-

ture at the low-energy edge of the low-temperature absorption spectrum. According to this interpretation, the absorption peaks at higher energy arose from phonon-assisted transitions in which the emission of one, two, or three phonons of the ZnS lattice accompanied the electronic transition. Subsequently, however, Slack and O'Meara² observed the corresponding ${}^5T_2 \rightarrow {}^5E$ luminescence at liquid-helium temperature and found that the only vibronic sidebands accompanying the zero-phonon emission lines were those corresponding to the emission of one phonon. Since the absence of two- and three-phonon sidebands in the luminescence spectrum is inconsistent with the presence of strong peaks of this type in absorption, the previously proposed interpretation